

PACS numbers: 42.62.Cf; 47.20.Ma
DOI: 10.1070/QE2009v039n04ABEH013798

Solidification structures on carbon materials surface-melted by repetitive laser pulses

D.V. Abramov, S.M. Arakelyan, S.V. Kutrovskaya, A.O. Kucherik, V.G. Prokoshev

***Abstract*. The solidification morphology of carbon materials surface-melted by laser radiation at atmospheric pressure is studied. Electron microscopy results indicate that melt solidification is accompanied by the formation of surface microstructures, presumably due to the Rayleigh – Taylor instability in the molten carbon. The instability increment and surface tension coefficient of molten carbon are estimated, and the penetration of carbon vapour into the melt during one laser pulse is examined using numerical simulation.**

Keywords: *carbon melting, Rayleigh – Taylor instability, electron microscopy*.

1. Introduction

There are various opinions about the mechanism of carbon melting at atmospheric pressure [1 – 3]. In a recent study [4], the use of a laser diagnostics system enabled real-time observation of carbon melting. Examination of surface morphology after laser heating provides greater insight into the processes in the modified zone [5].

In this paper, we report an electron-microscopic study of laser surface melted carbon and graphite samples. Characteristic solidification microstructures on carbon surfaces were detected in the irradiated region (the size of the same order as the spot size of the laser beam) and at its boundary. The nature and arrangement of the solidification structures observed on the sample surface suggest that they result from the development of Rayleigh – Taylor instability in liquid carbon.

2. Experimental

Glassy carbon and pyrolytic graphite samples were exposed to 2-ms, 1.06-μm Nd : YAG laser pulses at a repetition rate of 150 Hz. The laser spot size on the sample surface was varied from 100 to 400 μm, and the average incident power, from 10 to 100 W. The power density incident on the sample surface was up to 10^7 W cm^{-2}, and the laser exposure time was $t = 1 - 10$ s.

D.V. Abramov, S.M. Arakelyan, S.V. Kutrovskaya, A.O. Kucherik, V.G. Prokoshev Vladimir State University, ul. Gor'kogo 87, 600000 Vladimir, Russia; e-mail: kucherik@vlsu.ru

Received 17 January 2008; revision received 9 September 2008
Kvantovaya Elektronika **39** (4) 333 – 336 (2009)
Translated by O.M. Tsarev

After laser heating and melting, the sample surface was examined by scanning electron microscopy (SEM) on a Quanta 200 3D (digital images with a magnification of up to 100 000$^{\times}$ and spatial resolution of 3.5 nm).

3. Results

Laser heating of the surface of carbon materials produces liquid carbon in the melt pool [4]. The hydrodynamic processes that occur in the surface region under laser irradiation depend on the nature of the material and experimental conditions. Characteristically, laser-induced surface melting is evidenced by a solidified melt droplet in the central part of the crater (such droplets were observed only on the surface of glassy carbon and were probably due to the gas penetration into the originally nonporous material during melting because of the developing hydrodynamic instabilities and to the associated expansion of the material on solidification) (Fig. 1a), by regularly shaped, conical pores (Fig. 1b) in the surface layer of both materials (glassy carbon and pyrolytic graphite) and by spiral structures (Fig. 1c) and even solidified melt splashes (Fig. 1d), which cannot be produced by solid-state processes, on the pyrolytic graphite samples.

The formation of a periodic array of micropores in a limited zone leads us to assume that, during laser irradiation, the Rayleigh – Taylor instability develops in the melt pool. Such instabilities appear at the interface between two fluids of different densities when the heavier fluid is above the lighter fluid and there is an initial perturbation [6]. In the general case, perturbation ξ can be represented by capillary waves

$$\xi = \frac{\xi_0}{2} e^{\gamma t} \cos kx. \tag{1}$$

Here, γ is the instability increment, which can be determined as

$$\gamma = \left[\frac{ak(\rho_2 - \rho_1)}{\rho_1 + \rho_2}\right]^{1/2}, \tag{2}$$

where a is the acceleration of the interface of two liquids; $k = 2\pi/\lambda$ is the wave number (λ is the surface perturbation wavelength); ρ_2 is the density of the heavier fluid (carbon melt); and ρ_1 is the density of the lighter fluid (vapour).

In the system under consideration, where instability develops in the laser heating zone on the surface of a carbon-containing material, the heavier fluid (melt) is, on

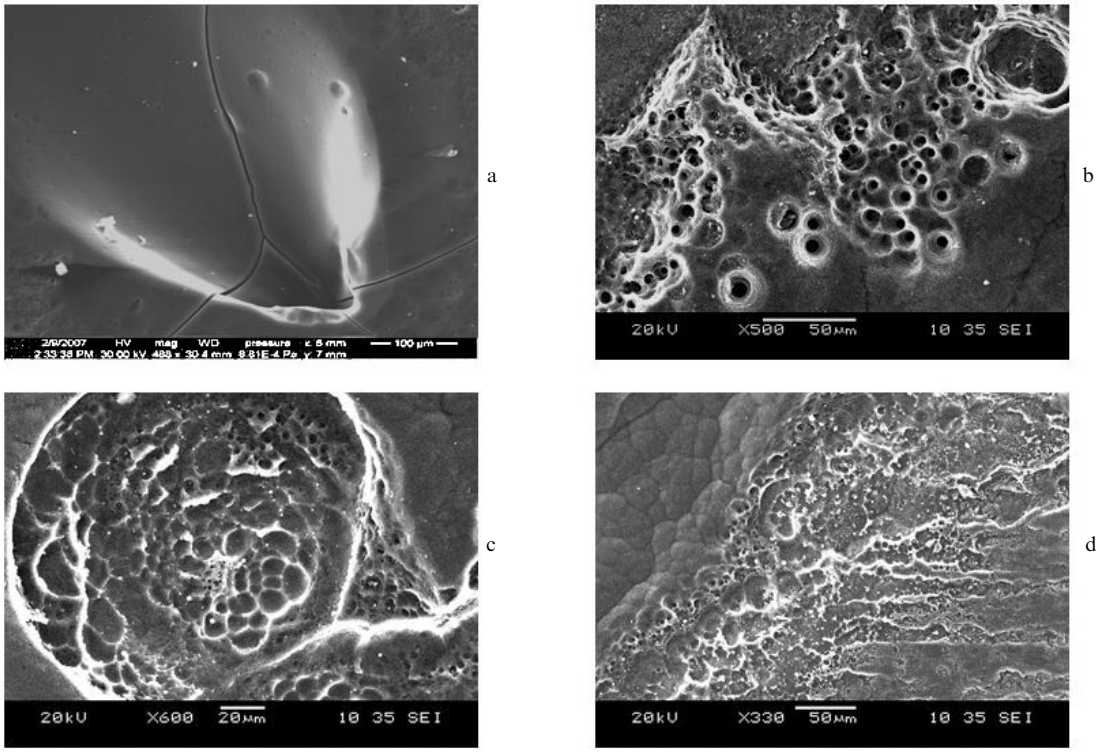

Figure 1. SEM images of sample surfaces: (a) solidified bump in the central part on the glassy-carbon surface; (b) regularly shaped, conical pores; (c) solidified spiral structure; (d) melt splashes.

the contrary, below the lighter fluid (carbon vapour), but the back pressure exerted by the erosion plume, located just above the zone being irradiated, accelerates the lighter fluid towards the surface, leading to interpenetration of the two fluids by virtue of the Rayleigh–Taylor instability [6] (Fig. 2a).

The acceleration of the interface between the liquid and vapour phases of carbon can be estimated as reported in Ref. [6] and, under the experimental conditions of this study, is $\sim 10^3$ m s^{-2}. The instability increment γ at this acceleration is 10^5 c^{-1}.

From Eqn (2) it readily follows that there is a minimum wavelength, λ_m, which corresponds to the largest instability increment, i.e. perturbation with this wavelength develops more rapidly than any other.

Surface images obtained after laser exposure (Fig. 2b) can be used to evaluate the wavelength of the initial perturbation: $\lambda_m = 5 \pm 0.5$ μm. Indeed, it can be seen that the average size of such perturbations ('pores') varies little from region to region. Thus, we are led to assume that the observed pore diameter is the characteristic size of the dominant initial perturbations, which meets the relation [7]

$$\lambda_m = \sqrt{6}\pi\zeta, \tag{3}$$

where

$$\zeta = \left(\frac{2\sigma}{\rho a}\right)^{1/2} \tag{4}$$

is the capillary constant and ρ is the density. From Eqn (3), the surface tension of liquid carbon can be estimated at 10^{-10} to 10^{-9} N m^{-1}.

4. Model

Assuming that the formation of pores on the glassy-carbon

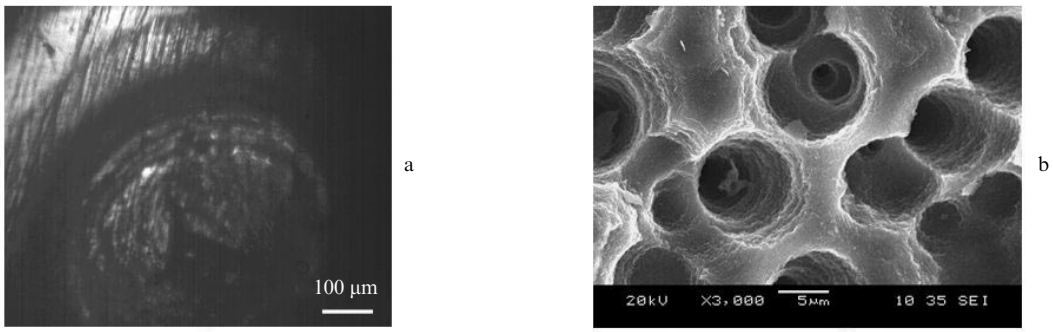

Figure 2. SEM images of sample surfaces: (a) periodic bright rings on the glassy-carbon surface; (b) conical structures on the pyrolytic-graphite surface.

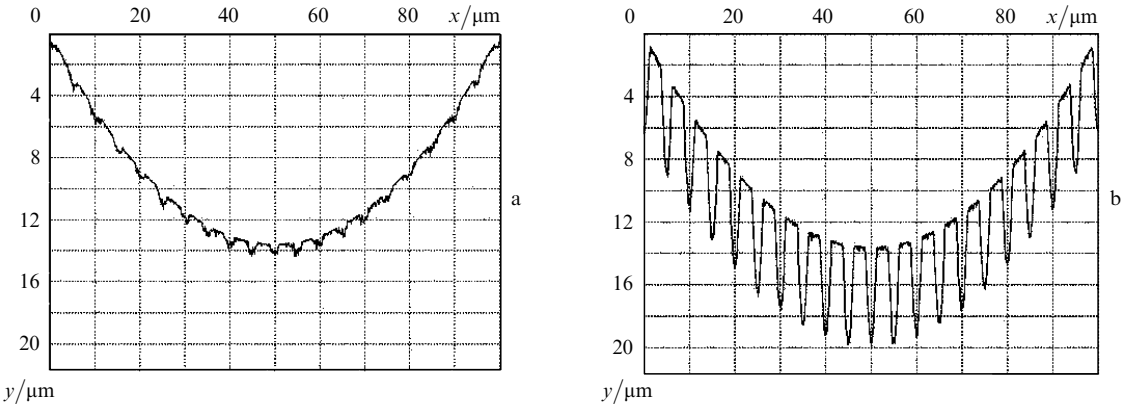

Figure 3. Initial perturbation produced by the vapour back pressure at the melt–vapour interface: $t = 0$ (a) and 10^{-4} s (b).

surface near the laser heating zone is due to the development of the Rayleigh–Taylor instability and subsequent melt solidification, we performed numerical simulation of carbon vapour penetration into the melt during one laser pulse. The initial perturbation at the interface between the melt and carbon vapour was taken in the form of waves given by Eqn (1). At the same time, since vapour penetration into the melt during instability development is a random process, a fractional Brownian motion model [7] was used near the interface in addition to a regular, exponentially growing periodic perturbation. The initial surface profile obtained with the present experimental parameters is shown in Fig. 3a. In 10^{-4} s, it experiences significant distortion (Fig. 3b).

Before the melt is forced out of the laser heating zone by the pressure of the erosion plume, solidification structures ~ 2 μm in depth may form.

5. Discussion

In the approach under consideration, instability at the interface between the melt and carbon vapour develops as follows: carbon melting by laser pulses [4, 5] is accompanied by active carbon vaporisation, leading to the

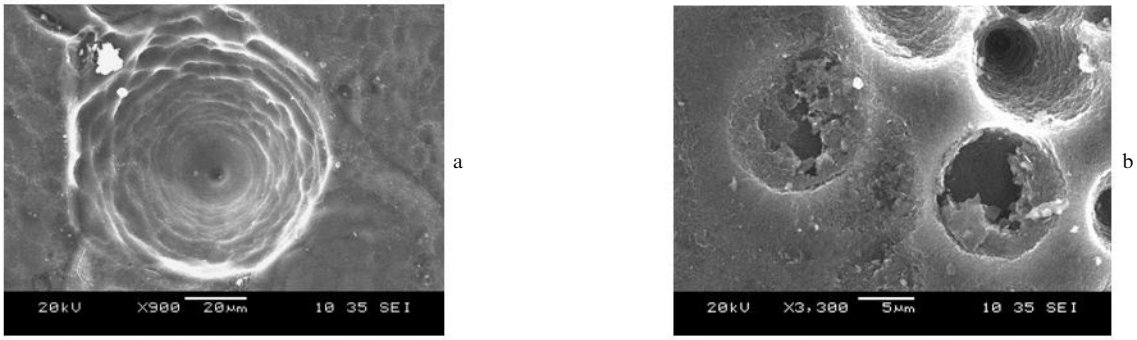

Figure 4. SEM images of bubbles on the pyrolytic-graphite surface: (a) closed bubble, (b) bubbles broken up after melt solidification.

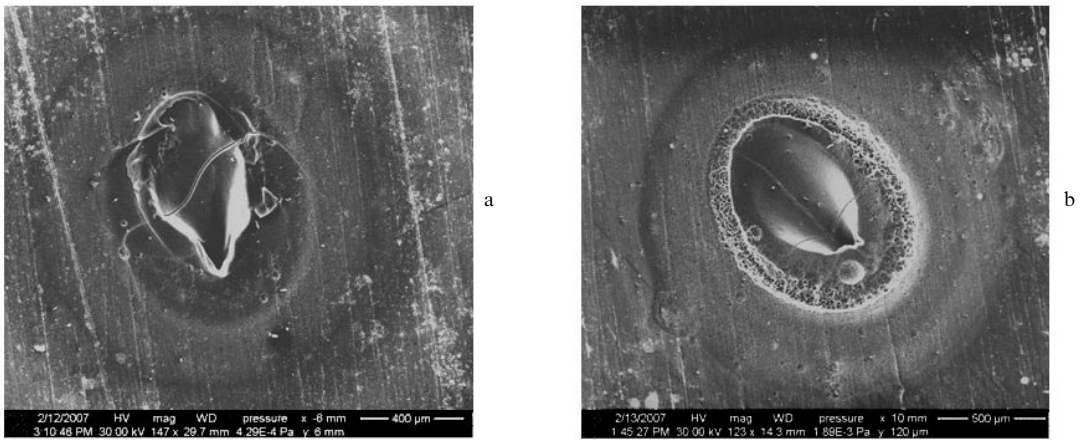

Figure 5. Typical view of the crater on the glassy-carbon surface: (a) solidified melt droplet in the central part and circular deposition zones, exposure time of 5 s or shorter; (b) the same features and a zone of conical structures (bubbles), exposure for more than 5 s.

formation of a dense erosion plume above the region being irradiated. With increasing the plume back pressure, the carbon vapour, which can be considered a lighter fluid, begins to penetrate into the melt, a heavier fluid [6]. The beginning of instability development at the interface is accompanied by motion of capillary waves (Fig. 4a), which subsequently decay, and more active interpenetration of the fluids begins, leading to the formation of pores in the melt. Since the vapour back pressure forces the melt out of the laser heating region, after melt solidification pores are also present at the boundary of the crater (Fig. 4b).

Under nonlaminar flow conditions, a small gas volume may be encapsulated in the melt. Being outside the high vapour back pressure region (at the periphery of the crater), the gas rises to the surface. However, because of the rapid solidification of molten carbon (within 0.2 μs according to our experimental data), not all of the gas bubbles present in the near-surface region reach the surface. This gives rise to characteristic surface distortions in the form of hillocks (Fig. 4a) or shallow (compared to pores produced by high vapour pressure) pits. Characteristically, these latter have solidified flakes at their periphery (Fig. 4b).

The formation of vortex structures (Fig. 1c) may be due to the nonuniformity of the external vapour pressure or the rapid melt motion.

In addition, we found that, under the experimental conditions of this study, only after 5 s of laser exposure enough molten material was produced for detecting the Rayleigh – Taylor instability (Fig. 5).

6. Conclusions

The solidification morphology of laser-surface-melted carbon samples was studied by electron microscopy. The results indicate that the origin of the observed solidification structures can be understood in terms of pyrolytic graphite/glassy carbon melting at a near-atmospheric pressure. The likely mechanism behind the formation of solidification structures is the Rayleigh – Taylor instability of the melt in the laser heating region. Numerical simulation lends support to this mechanism of local instability development during one laser pulse. However, under the conditions of this study, a sufficient amount of the melt (certain exposure time) is needed to detect laser-induced surface hydrodynamic processes.

References

1. Whittaker A.G. *Science*, **200** (4343), 763 (1978).
2. Whittaker A.G. *Nature*, **276** (5689), 695 (1978).
3. Asinoskii E.I., Kirillin A.V., Kostanovskii A.V. *Usp. Fiz. Nauk*, **172** (8), 931 (2002).
4. Abramov D.V., Arakelyan S.M., Galkin A.F., Kvacheva L.D., Klimovskii I.I., Kononov M.A., Mikhailitsyn L.A., Kucherik A.O., Prokoshev V.G., Saranskii V.V. *Pis'ma Zh. Eksp. Teor. Fiz.*, **84** (5), 315 (2006).
5. Abramov D.V., Gerke M.N., Kucherik A.O., Kutrovskaya S.V., Prokoshev V.G., Arakelyan S.M. *Kvantovaya Elektron.*, **37** (11), 1051 (2007) [*Quantum Electron.*, **37** (11), 1051 (2007)].
6. Chivel' Yu.A. *Kvantovaya Elektron.*, **18** (10), 1218 (1991) [*Quantum Electron.*, **21** (10), 1104 (1991)].
7. Saranin V.A. *Ravnovesie zhidkostei i ego ustoichivost'* (Equilibrium of Fluids and Its Stability) (Moscow: Inst. Komp'yuternykh Iccledovanii, 2002).